Hysteresis in the Cell Response to Time-Dependent Substrate Stiffness

Achim Besser[†] and Ulrich S. Schwarz[†‡*]
[†]Bioquant and [‡]Institute for Theoretical Physics, University of Heidelberg, Heidelberg, Germany

ABSTRACT Mechanical cues like the rigidity of the substrate are main determinants for the decision-making of adherent cells. Here we use a mechano-chemical model to predict the cellular response to varying substrate stiffnesses. The model equations combine the mechanics of contractile actin filament bundles with a model for the Rho-signaling pathway triggered by forces at cell-matrix contacts. A bifurcation analysis of cellular contractility as a function of substrate stiffness reveals a bistable response, thus defining a lower threshold of stiffness, below which cells are not able to build up contractile forces, and an upper threshold of stiffness, above which cells are always in a strongly contracted state. Using the full dynamical model, we predict that rate-dependent hysteresis will occur in the cellular traction forces when cells are exposed to substrates of time-dependent stiffness.

Received for publication 13 January 2010 and in final form 1 April 2010.

*Correspondence: ulrich.schwarz@bioquant.uni-heidelberg.de

During the last decade, it has been shown that all adherent cell types sense and respond to mechanical cues in their environment, including substrate stiffness and prestress (1). For example, fibroblastlike cells adhere stronger to stiffer substrates, including decreased motility, increase in spreading area, and higher contractile forces. Most strikingly, the fate of stem cells can be controlled by substrate stiffness (2). It is becoming increasingly clear that mechanosensing by tissue cells is not based on the functioning of one particular molecular entity, but depends on the dynamical function of a mechanosensitive system whose main components are actomyosin force generation and signaling from cell-matrix adhesions (3). For example, all the described effects are abolished by inhibiting myosin II activity with blebbistatin or the Rho-pathway with C3-toxin. Here we perform a systems-level analysis of rigidity sensing by tissue cells taking into account both the mechanical and biochemical aspects.

Our model is sketched in Fig. 1 *a*. Cell mechanics is represented by a viscoelastic model for a stress fiber (SF), which is the most prominent feature of the actin cytoskeleton developed in cell culture on flat substrates. The parallel arrangement of elastic and viscous elements leads to a Kelvin-Voigt element—i.e., the SF behaves like a solid on long timescales. In addition to the passive viscoelastic stress, we account for active actomyosin contractility. The myosin forces are determined by a force velocity relation whose properties are modulated by biochemical signals diffusing in the cytoplasm. Therefore, actomyosin contractility may vary spatially along the fiber. In the continuum limit of many elements in series, we arrive at a continuous Kelvin-Voigt material governed by a partial differential equation with mixed derivatives, the stress fiber equation (4).

The forces generated in the SF are transmitted to integrin-based cell-matrix adhesions, so-called focal adhesions (FAs), where they trigger biochemical signals feeding back to the actin cytoskeleton. The main mechanism that has been suggested in this context is the force-induced activation of the Rho-signaling pathway through guanine nucleotide exchange factors that reside in FAs (3). Activation of RhoA leads to activation of the Rho-associated kinase (ROCK). Active ROCK is able to phosphorylate myosin light chain phosphatase (MLCP) to MLCP-P and thereby deactivates the phosphatase. MLCP and MLCP-P are freely diffusible in the cytoplasm and can reach the myosins in the SFs. Increased phosphorylation of MLCP to MLCP-P by ROCK thus effectively leads to increased phosphorylation of myosin light chain (MLC), increasing myosin contractility along the SFs. In our model, this signaling pathway is described by a system of reaction diffusion equations where each enzymatic step is described by Michaelis-Menten kinetics (4). The actomyosin force is assumed to activate the Rho-pathway with Michaelis-Menten kinetics. This is the simplest assumption given a linear increase in biochemical activity at small force and saturation at large force. The biochemical signal couples into the SF contraction mechanics via the force velocity relation of the myosin motors. In this way, a mechanical and biochemical positive feedback loop is closed (depicted in Fig. 1 *b*). The mechano-chemical model has been introduced before to describe inhomogeneous SF contraction upon myosin stimulation by the drug calyculin (4). To account for compliant substrates, we now appropriately modify the boundary conditions of the SF equation. In this situation, at each fiber end the traction forces F_t exerted by the SF have to be balanced by the elastic restoring forces of the substrate. The latter is modeled as a linear elastic spring of stiffness k_s. All model equations and parameter values are summarized in the Supporting Material.

Editor: Alexander Mogilner.

doi: 10.1016/j.bpj.2010.04.008

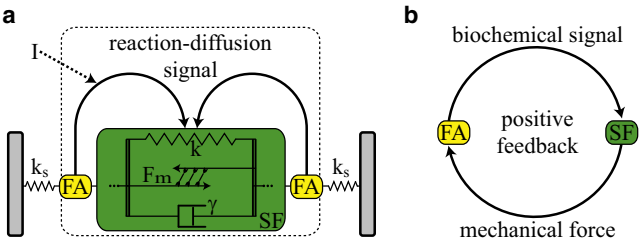

FIGURE 1 The mechano-chemical model: (*a*) The stress fiber (SF) is modeled as a continuous one-dimensional Kelvin-Voigt material (spring stiffness *k*, viscosity γ) that may locally contract due to actomyosin forces (F_m). Force-induced signaling at focal adhesions (FA) is described by a reaction-diffusion system (Rho-pathway). Substrate stiffness k_s and biochemical stimulation *I* (e.g., calyculin) are used as control parameters. (*b*) Higher forces on FAs increase Rho-signaling which, in turn, leads to higher myosin activation, thus closing a positive feedback loop.

BIFURCATION ANALYSIS

Motivated by their experimental relevance, we start with a bifurcation analysis with the nondimensional ratio of substrate and SF stiffness k_s/k and the stimulation strength I as control parameters. The parameter I accounts for the inhibitory effects of calyculin on MLCP: $I = 1$ corresponds to an unperturbed system and $I > 1$ ($I < 1$) leads to higher (lower) actomyosin activity. As state variable, we introduce the absolute value of the exerted traction forces, $F_t = |k_s u|$. An alternative is the substrate deformation u (see the Supporting Material for these results).

Fig. 2 shows the bifurcation diagram for the traction force F_t as a function of the stiffness ratio k_s/k for different values of the stimulation strength I. For each value of I, the upper blue and the lower red branch represents the stable fixed points for different values of the stiffness ratio k_s/k. The unstable branch is indicated as a dashed line. The S-shape of these curves demonstrates that the system is strongly bistable due to the positive feedback between force and signaling. The stable upper branch corresponds to a highly contractile cell whereas the stable lower branch corresponds to an inactive cell that fails to establish a contractile state. Both branches increase monotonically with substrate stiffness. However, the upper branch quickly saturates for high stiffness ratios. It can be deduced from Fig. 2 that for all considered values of I there exist a critical stiffness ratio, defined by the left bifurcation point, below which the upper stable branch vanishes. As a consequence, on very soft substrates, cells cannot establish a highly contractile state. Correspondingly, on the stiff side there exists a threshold above which unperturbed cells are always contractile.

By systematically sampling the two-dimensional parameter space, the stable and unstable branches become surfaces defined over the (k_s/k)–(I) plane (shown in Fig. 3). The two folds where the surface bends over itself define two bifurcation curves representing the two thresholds involved. Their projection on the parameter plane, shown as dashed lines, yields the stability diagram of the system. The curves divide the plane into three regions, namely inactive, contractile, or bistable. If the system is driven out of the bistable region by a parameter change, it can be forced to a sudden transition between the inactive and the contractile states. This prediction is consistent with the experimentally observed abrupt appearance of mature SFs in 3T3 fibroblasts if the substrate stiffness is increased beyond a threshold value of ≈ 3 kPA (5). Cells also spread faster on stiff substrates (5), and this corresponds to a faster buildup of forces as predicted by our model (see Fig. S3 in the Supporting Material). The course of spreading experiments is indicated by upward arrows in Fig. 2. However, they cannot reach the upper stable branch in the bistable region. Our results suggest that this state can be attained by stimulated cells after washout of calyculin (indicated by the *down arrows* in Fig. 2).

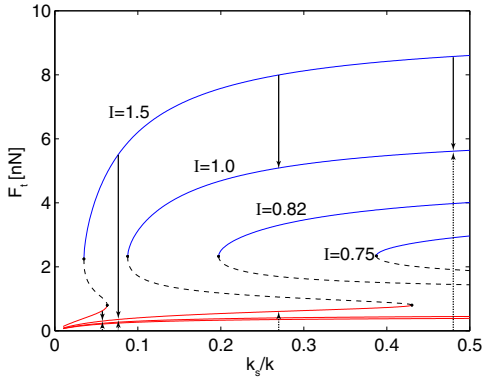

FIGURE 2 Bifurcation diagrams for the traction force F_t using the stiffness ratio k_s/k as control parameter and varying stimulation strength $I \in \{0.75, 0.82, 1.0, 1.5\}$. Shown are: stable upper branches (*blue*) that correspond to contractile states; stable lower branches (*red*) that correspond to inactive states; unstable branches (*dashed lines*); and saddle node bifurcation points (*black dots*). Upward and downward arrows illustrate spreading and calyculin washout experiments, respectively.

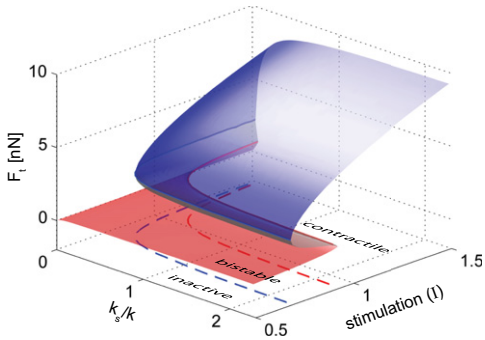

FIGURE 3 Two-parameter (stiffness ratio k_s/k, stimulation strength *I*) bifurcation diagram for the traction force F_t. Colored planes represent: stable upper branch (*blue*); stable lower branch (*red*); and unstable branch (*gray*). A stability diagram is constructed by projecting the two bifurcation curves (*red* and *blue solid lines*) onto the parameter plane (*dashed lines*), subdividing it in contractile, bistable, and inactive regions.

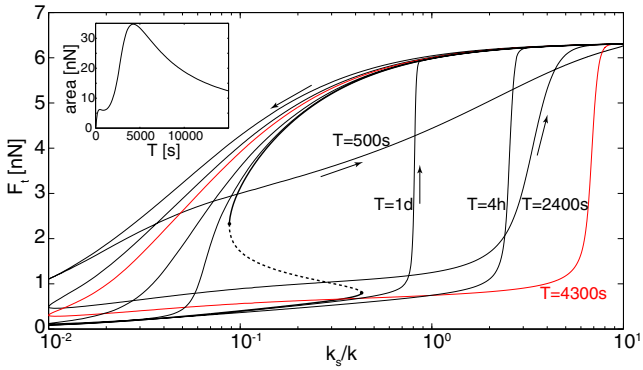

FIGURE 4 Time course of traction force F_t for cyclic varying substrate stiffness with period $T \in$ {500 s, 2400 s, 4300 s, 4 h, 1 d}, in the biochemically unperturbed case $I = 1.0$. The area of the hysteresis cycle as a function of the period (given as *inset*) reaches a maximum at $T = 4300$ s $\pm$ 100 s (*red curve*). The bifurcation diagram (*black lines*) is approached for $T \to \infty$. Arrows indicate cycling direction.

HYSTERESIS AND RATE EFFECTS

An important consequence of the bistability revealed by our bifurcation analysis is the existence of a hysteresis loop for cell adhesion. To construct such a hysteresis cycle, cells had to be prepared on stiff substrates in the highly contractile state (compare Fig. 2). By reducing the substrate stiffness sufficiently slowly, such that the system can adapt and remain in a quasisteady state, it will follow the upper stable branch until it reaches the left bifurcation point. Here, the upper branch becomes unstable and the system is forced into the inactive state. When the control parameter is increased again, the system will stay on the lower branch until it reaches the right bifurcation point, where the lower branch becomes unstable. Thus, the system is finally forced again onto the upper branch and the hysteresis cycle is closed.

The ideal hysteresis scenario is expected to occur only for very slow changes in stiffness. In experiments, rate effects might occur. To analyze this situation theoretically, we now can take full advantage of our dynamical model. We have simulated this experiment with COMSOL Multiphysics for a stiffness ratio $k_s(t)/k$, which oscillates sinusoidally between 0.01 and 10.0 with different periods T. This stiffness range is chosen such that it covers the bistable region. The resulting time courses for the traction forces are shown in Fig. 4. As an inset we show the encircled hysteresis area as a function of the period T. For very large periods ($T = 1$ d), the system follows essentially the bifurcation diagram. The area of the hysteresis cycle first increases with the frequency and reaches a maximum for $T =$ 4300 s (*red curve* in Fig. 4). For very high frequencies, the hysteresis cycle tightens up again as the period of the mechanical input becomes smaller than the relaxation time of the biochemical system. In this case, the biochemical part of the system conserves the initial activation and thus, the system can maintain higher forces on soft substrates, leading to a rather flat time course of the traction forces (compare $T = 500$ s in Fig. 4).

CONCLUSIONS AND OUTLOOK

A bifurcation analysis of our dynamical systems model showed that the described positive mechano-chemical feedback cycle leads to bistability for contraction as a function of substrate stiffness. This readily explains the experimentally observed abrupt change in the morphology and contractility of fibroblastlike cells at a rigidity threshold. Due to its dynamical nature, our model also allows us to predict the different hysteresis curves expected for different frequencies of dynamically changing substrate stiffness. Recently, different experimental setups have been introduced, which make cell experiments on substrates with time-dependent stiffness possible. Hydrogels made from thiolated hyaluronic acid and polyethylene glycol diacrylate exhibits a time-dependent increase in the Young modulus (6). The stiffness can be reduced again by breaking formed disulfide bonds with dithiothreitol. Alternatively, micromanipulation systems like atomic force microscopes or microplates can be used to mimic compliant substrates through an electronic feedback system (7).

Our analysis demonstrates that such dynamical protocols open up a new dimension of controlling cell behavior through physical cues. Here, we have restricted our treatment to a single fiber as a paradigm as to how cells couple biochemistry and mechanics. Future work should also address how different fibers interact with each other. Fibers in the same cell should share the biochemical input through diffusion fields, while all fibers (including those from other cells) might interact mechanically through a compliant substrate.

SUPPORTING MATERIAL

Four equations, two tables, and three figures are available at http://www.biophysj.org/biophysj/supplemental/S0006-3495(10)00440-6.

ACKNOWLEDGMENTS

We thank F. Rehfeldt for helpful discussions.

This work was supported by the cluster of excellence CellNetworks at the University of Heidelberg.

REFERENCES and FOOTNOTES

1. Janmey, P. A., J. P. Winer, …, Q. Wen. 2009. The hard life of soft cells. *Cell Motil. Cytoskeleton.* 66:597–605.
2. Discher, D. E., D. J. Mooney, and P. W. Zandstra. 2009. Growth factors, matrices, and forces combine and control stem cells. *Science.* 324:1673–1677.
3. Geiger, B., J. P. Spatz, and A. D. Bershadsky. 2009. Environmental sensing through focal adhesions. *Nat. Rev. Mol. Cell Biol.* 10:21–33.
4. Besser, A., and U. S. Schwarz. 2007. Coupling biochemistry and mechanics in cell adhesion: a model for inhomogeneous stress fiber contraction. *N. J. Phys.* 9:425.
5. Yeung, T., P. C. Georges, …, P. A. Janmey. 2005. Effects of substrate stiffness on cell morphology, cytoskeletal structure, and adhesion. *Cell Motil. Cytoskeleton.* 60:24–34.
6. Engler, A. J., F. Rehfeldt, …, D. E. Discher. 2007. Microtissue elasticity: measurements by atomic force microscopy and its influence on cell differentiation. *Methods Cell Biol.* 83:521–545.
7. Mitrossilis, D., J. Fouchard, …, A. Asnacios. 2009. Single-cell response to stiffness exhibits muscle-like behavior. *Proc. Natl. Acad. Sci. USA.* 106:18243–18248.